

# OPTIMIZATION OF POSITRON CAPTURE IN NLC\*

Yuri K. Batygin, SLAC, Stanford, CA 94309, USA

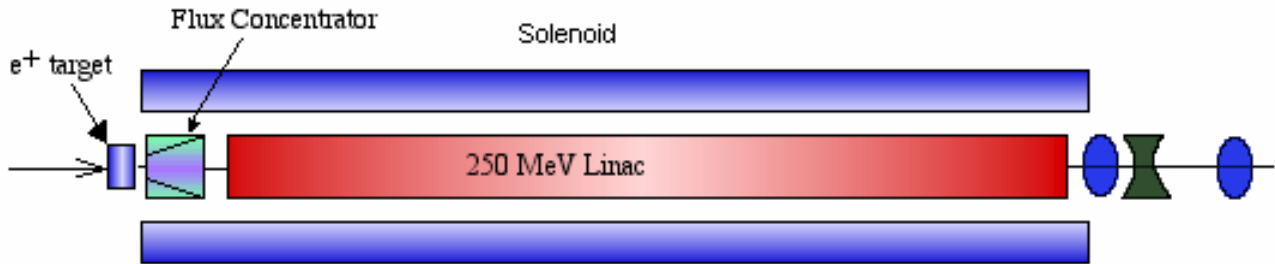


Figure 1: Layout of the NLC positron injector.

## Abstract

In the Next Linear Collider design [1], the positron capture system includes a positron production target, followed by a short solenoid with a strong magnetic field (flux concentrator), a 250 MeV linac with solenoidal focusing, a 1.73 GeV linac with quadrupole focusing and an energy compressor system before injection into the positron pre-damping ring (see Fig. 1 for initial part of collector). Two schemes for positron production have been studied: (i) a conventional approach with a 6.2 GeV electron beam interacting with a high-Z target and (ii) polarized positron production using polarized photons generated in a helical undulator by a 150 GeV electron beam which then interact with a positron production target. The capture system has been optimized to insure high positron yield into the 6-dimensional acceptance of the pre-damping ring. As a result of these optimization studies, the positron yield in the conventional scheme has been increased from 1.0 to at least 1.5 and capture for the polarized positron scheme from 0.25 to 0.30 while maintaining 60% positron polarization.

## POSITRON YIELD, CAPTURE AND POLARIZATION

Generated positron beam is characterized by large value of beam emittance and wide energy spread (see Fig. 2). At the time of injection into the pre-damping ring,

positron capture is restricted by the acceptance of the pre-damping ring. It is convenient to select an energy-invariant 6-dimensional phase space volume and compare positron capture within this volume at different stages of the injector. To provide positrons injection into the pre-damping ring, the normalized positron beam emittance is selected to be  $\epsilon_x, \epsilon_y \leq 0.03 \pi \text{ m rad}$  and the energy spread  $\Delta E/E = \pm 1\%$  at the injection energy of 1.98 GeV (see Fig. 3).

For analysis, we use several criteria, which characterize efficiency of positron collection. Positron capture is a ratio of the number of positrons within invariant 6-dimensional volume,  $N_{e^+}$ , to the number of positrons generated after the positron production target,  $N_{e^+, \text{target}}$ . Positron yield is defined as a ratio of accepted positrons into the pre-damping ring at the energy of 1.98 GeV to the number of incident electrons,  $N_e$ , or to the number of incident photons,  $N_\gamma$ , interacting with the target. Longitudinal polarization of a positron beam,  $\langle P_z \rangle = \langle S_z P \rangle$ , is an average of the product of the longitudinal component of positron spin vector,  $S_z$ , and the value of positron polarization,  $P$ , over all positrons.

Table 1 illustrates dependence of positron yield in the conventional production scheme with respect to different values of 6-dimensional acceptance of the pre-damping ring.

Table 1: Positron yield at 1.98 GeV as a function of 6D acceptance.

6-D phase space	$\epsilon_x, \epsilon_y < 0.03 \pi \text{ m rad}, \Delta E/E = 2\%$	$\epsilon_x, \epsilon_y < 0.045 \pi \text{ m rad}, \Delta E/E = 2\%$	$\epsilon_x, \epsilon_y < 0.06 \pi \text{ m rad}, \Delta E/E = 2\%$	$\epsilon_x, \epsilon_y < 0.03 \pi \text{ m rad}, \Delta E/E = 4\%$	$\epsilon_x, \epsilon_y < 0.045 \pi \text{ m rad}, \Delta E/E = 4\%$	$\epsilon_x, \epsilon_y < 0.06 \pi \text{ m rad}, \Delta E/E = 4\%$
Positron yield	1.01	1.26	1.36	1.25	1.55	1.69

\*Work supported by the Department of Energy Contract No. DE-AC03-76SF00515

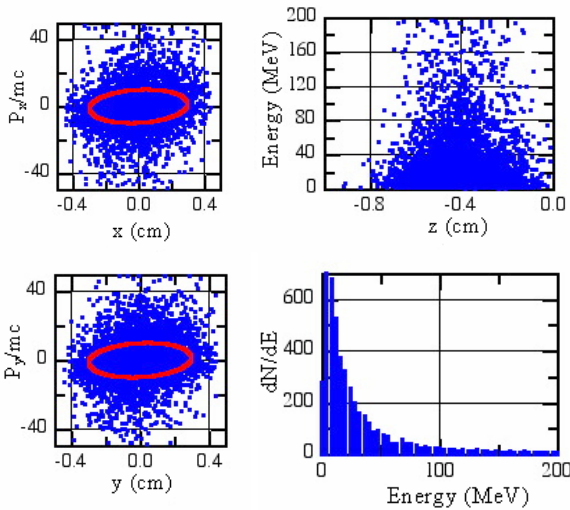


Figure 2: (Blue) initial distribution of positrons generated by a 6.2 GeV electron beam after interaction with a 4.5 RL W-Re target; (Red) area of  $0.03 \pi$  m rad.

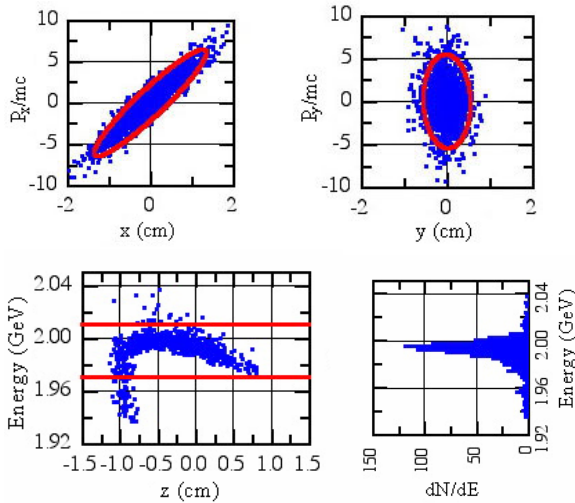


Figure 3: (Blue) distribution of positrons at 1.98 GeV; (Red) emittance area of  $0.03 \pi$  m rad and  $\Delta E/E=2\%$ .

### POSITRON TRANSMISSION TROUGH FLUX CONCENTRATOR

According to the design, the positron production target is surrounded by a tapered solenoidal magnetic field of  $B_t = 1.2$  Tesla followed by a strong magnetic field of flux concentrator with a total peak field of  $B_{FC} = 6.4$  Tesla. The sharp change in the magnetic field at the injection is a barrier for low-energy positrons. Fig. 4 illustrates the magnetic field profile of the flux concentrator and distribution of positrons after injection into flux concentrator. Fig. 4 features high-energy positrons which passed through the field and low-energy positrons reflected from the field. The barrier for low-energy positrons can be removed if the positron production target is placed inside a strong magnetic field

Table 2: Positron capture after the flux concentrator (FC) and after acceleration up to 250 MeV as function of FC magnetic field configuration

$B_z$ at target, Tesla	FC field $B_z(z)$ , Tesla	Aperture along FC, cm	Capture after FC	Capture at 250 MeV
1.2	6.4...0.5	0.5...2	0.29	0.24
6.4	6.4	0.5...2	0.42	0.09
6.4	6.4	2	0.42	0.09
6.4	6.4...0.5	0.5...2	0.39	0.33

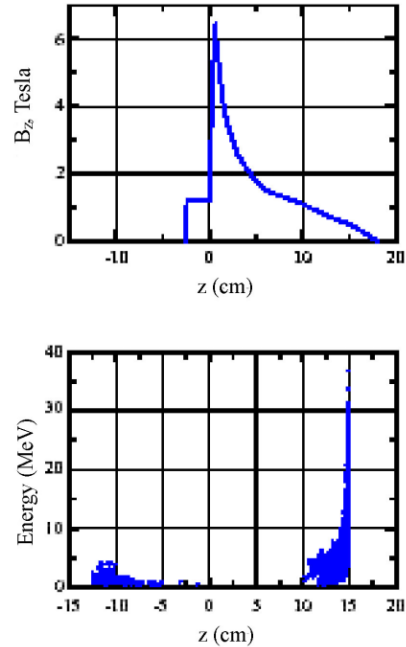


Figure 4: (Top) magnetic field profile in flux concentrator; (Bottom) distribution of positrons from 10.7 MeV  $\gamma$ -flux after injection into flux concentrator.

of flux concentrator [2]. Table 2 contains results of a simulation of positron capture at different configurations of the magnetic field of the flux concentrator. Moving the target inside strong magnetic field increases positron capture by a factor of 1.37 (compare the first and the last lines in Table 2). Utilizing a flux concentrator with a constant magnetic field of 6.4 Tesla results in better transmission of positrons through the magnet. However, because of the mismatching of the constant field of 6.4 Tesla with the 0.5 Tesla focusing field of the 250 MeV linac, transmission of accelerated positrons in this case drops seriously.

### DECELERATION OF POSITRONS

After the flux concentrator, positron distribution has a tail created by low-energy positrons (see right side distribution of positrons in Fig. 4). An effective method of increasing of positron capture was proposed in Ref. [3]. It is based on the fact, that this specific positron distribution is close to the shape of longitudinal phase-

Table 3: Positron yield with respect to incident  $\gamma$  – flux

Energy of 1 <sup>st</sup> harm. cutoff, MeV	Yield at the target	Capture at 1,9 GeV	Yield at 1.9 GeV
10.7	0.029	0.20	$5.8 \times 10^{-3}$
30	0.11	0.058	$6.4 \times 10^{-3}$
60	0.17	0.026	$4.4 \times 10^{-3}$

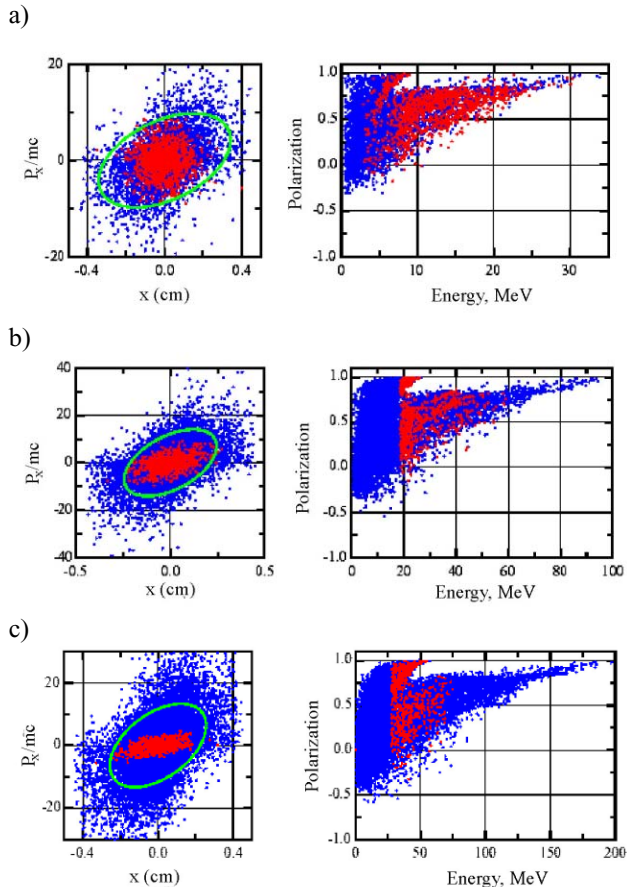


Figure 5: (Blue) initial distribution of polarized positrons, generated by: (a) 10.7 MeV  $\gamma$ -flux, (b) 30 MeV  $\gamma$ -flux, (c) 60 MeV  $\gamma$ -flux, (red) positrons accepted at 1.98 GeV, (green) area of  $0.03 \pi$  m rad.

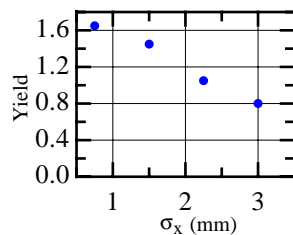


Figure 6: Positron yield vs. transverse electron bunch size (bunch length  $\tau = 4$  ps, target Hg, 4 RL).

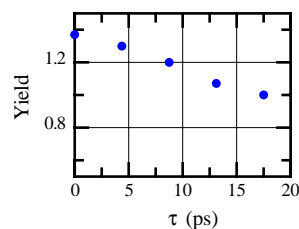


Figure 7: Positron yield vs. bunch length ( $\sigma_x = 1.6$  mm, target W-Re, 4.5 RL).

space orbits of linac. Particles, originally placed along the phase-space trajectory, will remain at the trajectory. As shown in Ref. [3], particles, after deceleration, will be compressed and accelerated as a short bunch with better transmission efficiency.

Simulations indicate that this process of beam bunching is accompanied with an increase of transverse emittance of a beam. As a result, the total number of positrons accepted at 1.98 GeV within the normalized emittance of  $\epsilon_x, \epsilon_y \leq 0.03 \pi$  m rad and the energy spread of  $\Delta E/E = 2\%$ , remains the same. However, if transverse acceptance is allowed to be increased by  $0.06 \pi$  rad, the number of accepted positrons due to deceleration-bunching increases by a factor of 1.13.

### POSITRON YIELD AS A FUNCTION OF ENERGY OF POLARIZED $\gamma$ -FLUX

Fig. 5 and Table 3 contain results of capture of polarized positrons created by the K=1, helical undulator spectrum with first harmonic cutoff energies of 10.7 MeV, 30 MeV and 60 MeV. With an increase of energy of  $\gamma$ -flux, positron yield at the target increases. However, increase of the energy of incoming photons results in wider energy spectrum of outgoing positrons. From Fig. 5 it follows that the distribution of positron polarization as a function of energy remains qualitatively the same, but is scaled to a wider energy interval. As a result, positron capture drops with increase of energy of  $\gamma$ -flux. Positron yield at 1.9 GeV (last column in Table 3) is a product of that at the target (2<sup>nd</sup> column) and of the value of capture (3<sup>rd</sup> column). As a result, the positron yield has a maximum at the energy of  $\gamma$ -flux of 30 MeV while the final beam polarization is 60%.

### POSITRON YIELD AS A FUNCTION OF INCIDENT ELECTRON BUNCH SIZES

Reduction of sizes of the incident electron beam results in a decrease of generated positron beam emittance in the conventional positron production scheme. Nominal value of a transverse electron beam size is  $\sigma_x = 1.6$  mm and that of a bunch length is  $\tau = 17$  ps. Incident electron bunch can be made more compact by utilizing traditional compression scheme. Figs. 6, 7 indicate that positron yield can be increased by a factor of 1.37 using electron bunch with smaller sizes.

### REFERENCES

- [1] Zeroth-Order Design Report for the Next Linear Collider, SLAC Report 474 (1996).
- [2] V.Belov et al., Proceedings of the 2001 Particle Accelerator Conference, Editors P.Lucas, S.Webber (2001), p. 1505.
- [3] B.Aune, R.H.Miller, Proceedings of the 1979 Linear Accelerator Conference, Edited by R.L.Witkov, BNL 51134 (1979), p. 440.